THE ASTROPHYSICAL JOURNAL, 251:364–373, 1981 December 1

ENERGETIC ELECTRONS AND PLASMA WAVES ASSOCIATED WITH A SOLAR TYPE III RADIO BURST

R. P. LIN AND D. W. POTTER
Space Sciences Laboratory, University of California, Berkeley
D. A. GURNETT
Department of Physics and Astronomy, University of Iowa
AND
F. L. SCARF
TRW Defense and Space Systems, Redondo Beach, California
Received 1981 February 23; accepted 1981 June 4

ABSTRACT

We present detailed in situ observations from the *ISEE 3* spacecraft of energetic electrons, plasma waves, and radio emission for the type III solar radio burst of 1979 February 17. The reduced one-dimensional distribution function $f(v)$ of the electrons is constructed as a function of time. Since the faster electrons arrive before the slower ones, a bump on tail distribution is formed which is unstable to the growth of Langmuir waves. The plasma wave growth computed from $f(v)$ agrees well with the observed onset of the Langmuir waves, and there is qualitative agreement between variations in the plasma wave levels and in the development of regions of positive slope in $f(v)$. The evolution of $f(v)$, however, predicts far higher plasma wave levels than those observed. The maximum levels observed are about equal to the threshold for nonlinear wave processes, such as oscillating two-stream instability and soliton collapse. Also, the lack of obvious plateauing of the distribution suggests that the observed waves have been removed from resonance with the beam electrons. Finally, the plasma waves are observed to be highly impulsive in nature.

The onset of the 56 kHz radio emission, identified by its lack of directivity as that produced in situ near 1 AU, precedes the plasma wave onset by $\sim$ 20 minutes. This delay raises serious questions about the hypothesis of the generation of type III radio emission from the plasma waves.

Subject headings: plasmas — Sun: radio radiation

I. INTRODUCTION

Type III solar radio bursts are produced by fast particles ejected from the Sun. The bursts are characterized by a rapid drift from high to low frequency which is attributed to the decreasing electron plasma frequency f_{p-} encountered by the fast particles as they move outward through the solar corona. The primary radiation is believed to occur at either the fundamental, f_{p-}, or the harmonic, $2f_{p-}$, of the local electron plasma frequency. Several years ago, it was established that electrons with energies from a few keV to a few tens of keV, often from solar flares, are primarily responsible for the type III radio emission (Lin 1970, 1974; Alvarez, Haddock, and Lin 1972; Frank and Gurnett 1972; Lin, Evans, and Fainberg 1973). More recently, Gurnett and Anderson (1976, 1977) have also observed intense electron plasma oscillations in association with type III radio bursts, apparently confirming a basic mechanism first proposed by Ginzburg and Zheleznyakov (1958). In this mechanism, which has been further refined by numerous investigators, including, for example, Tidman, Birmingham, and Stainer (1966), Kaplan and Tsytovich (1968), Papadopoulos, Goldstein, and Smith (1974), Smith (1977), and Nicholson *et al.* (1978), type III radio bursts are produced by a two-step process in which intense electrostatic electron plasma oscillations are first excited by a two-stream instability caused by the solar fast electrons, and then these plasma oscillations decay into electromagnetic radiation because of nonlinear interactions.

Sturrock (1964) pointed out that in a homogeneous beam-plasma model the fast particle stream, i.e., a bump on tail distribution (see Fig. 1), is so rapidly diffused in velocity space by the intense plasma oscillations that a coherent stream would only be able to travel a few kilometers from its source before it is plateaued. A major question then for type III burst theory is: What allows the stream to propagate from the Sun to well past 1 AU, as observed? Observations show that the stream is highly inhomogeneous with the bump on tail distribution produced by the faster electrons running ahead of the slower ones. At a given distance from the fast particle source, the bump in the distribution moves from high to low velocity with time. Thus, one possibility is that plasma waves produced by the positive slope portion of the distribution may not build up to sufficient amplitudes to interact with the bump before the bump has moved to lower velocities. Also, the plasma waves produced with a given phase velocity at time t_1 by a positive slope may be reabsorbed at a later time t_2 when a negative slope is present. Several model calculations suggest that the

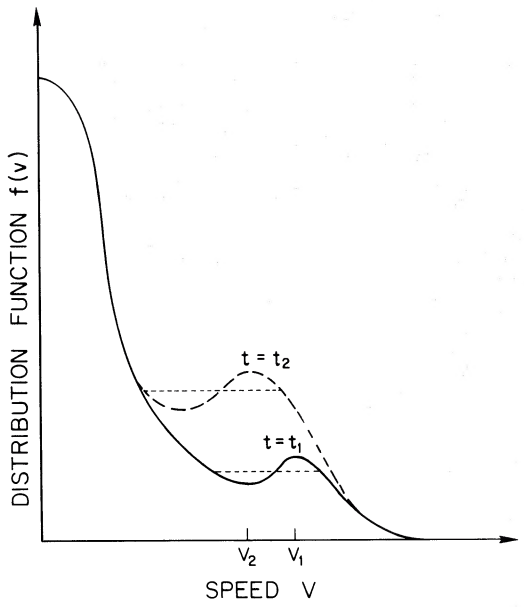

FIG. 1.—For the distribution function at t_1 (*solid line*), waves with phase velocity between V_2 and V_1 grow since the slope is positive. Eventually these waves would plateau the distribution. If the bump on tail distribution is produced by the faster electrons arriving from the source before the slower ones, then the bump will move to lower velocities with time (t_2; *dashed curve*).

quasi-linear relaxation (plateauing) will occur, but reabsorption of the plasma waves is important in enabling the stream to propagate large distances without catastrophic energy loss (Magelssen and Smith 1977; Takakura and Shibahashi 1976).

Another possibility is that various nonlinear wave-wave interactions may be important in shifting the plasma waves to different wave numbers where they are no longer resonant with the beam electrons (Papadopoulos, Goldstein, and Smith 1974; Bardwell and Goldman 1976; Nicholson *et al.* 1978). This would allow the electrons to travel large distances without catastrophic energy loss (Smith, Goldstein, and Papadopoulos 1979; Goldstein, Smith, and Papadopoulos 1979).

In this paper, we present an analysis of a type III burst event for which exceptionally clear and detailed measurements of the radio emission, electron plasma oscillations, and energetic electrons are available. For the first time, observations are obtained with sufficient sensitivity and energy and angular resolution to construct the distribution function of the electrons. These distributions provide important information on the plasma processes that are occurring. The energetic electron measurements show how these solar particles control the onset and growth of the electron plasma oscillations. Quantitative comparisons of the electron and plasma wave data indicate that some process, perhaps one of the nonlinear processes discussed above, is removing the waves from resonance with the electrons. The timing of the onset of the plasma oscillations in relation to the type III radio emission, however, raises several important questions concerning the mechanism by which the radio emission is generated.

The event analyzed occurred on 1979 February 17 and was detected by several spacecraft, including *ISEE 1*, *2*, and *3*, *Helios 2*, and *IMP 8*. The primary data used in this study were obtained from the *ISEE 3* spacecraft, which at the time of this event was located in the solar wind approximately 259 R_e upstream from the Earth. The radio and plasma wave measurements are from the joint TRW-JPL-Iowa plasma wave instrument on *ISEE 3*, and the energetic electron measurements are from the University of California, Berkeley, solar electron instrument on *ISEE 3*. Other measurements used are from the joint Iowa-TRW-JPL plasma wave instrument on *ISEE 1* and the University of Iowa plasma wave instruments on *Helios 2* and *IMP 8*. For a description of these instruments see Scarf *et al.* (1978), Anderson *et al.* (1978), Gurnett *et al.* (1978*b*), Gurnett and Anderson (1977), and Gurnett (1974).

II. CHARACTERISTICS OF THE 1979 FEBRUARY 17 EVENT

The event of interest occurred from about 1930 to 2300 UT on 1979 February 17. A frequency-time spectrogram of the radio emissions detected by *ISEE 1* during this period is shown in Figure 2. Two type III radio bursts are evident in this spectrogram, the first starting at about 1815 UT, and the second, the one of interest, starting at about 1930 UT. Although several solar flares were observed from the ground during this period (Solar Geophysical Data 1979), all were located near or east of the central meridian and are unlikely to be associated with these events. Because of the Archimedian spiral form of the interplanetary magnetic field (Parker 1958), it is most likely that the originating flare occurred behind the west limb of the Sun, possibly from the McMath plage region 15807 at 15° N latitude, which had been quite active for several days before disappearing behind the west limb on February 16. This identification of the flare position is given added support by the stereoscopic *ISEE 1*, *IMP 8*, and *Helios 2* radio direction finding measurements. Although the exact trajectory of the burst is somewhat uncertain because of the unfavorable viewing geometry, both the *ISEE 1* and *Helios 2* measurements show that the burst centroid originated near the west limb of the Sun and passed well to the west of the Earth.

The simultaneous electric field and low-energy electron intensities observed by *ISEE 3* during this event are illustrated in Figure 3. The top panel shows the electric field intensities in four frequency channels from 17.8 to 100 kHz. The black areas give the electric field intensities averaged over intervals of 32 s, and the solid lines give the peak electric intensities over corresponding intervals. The smooth intensity variations characteristic of a type III radio burst, consisting of a rapid rise followed by a slow monotonic decay, are clearly evident in the 56.2 and 100 kHz channels. Spin modulation is observed for the 100 kHz emission but is absent at 56.2 kHz. This lack of directivity suggests that the 56.2 kHz radio emission

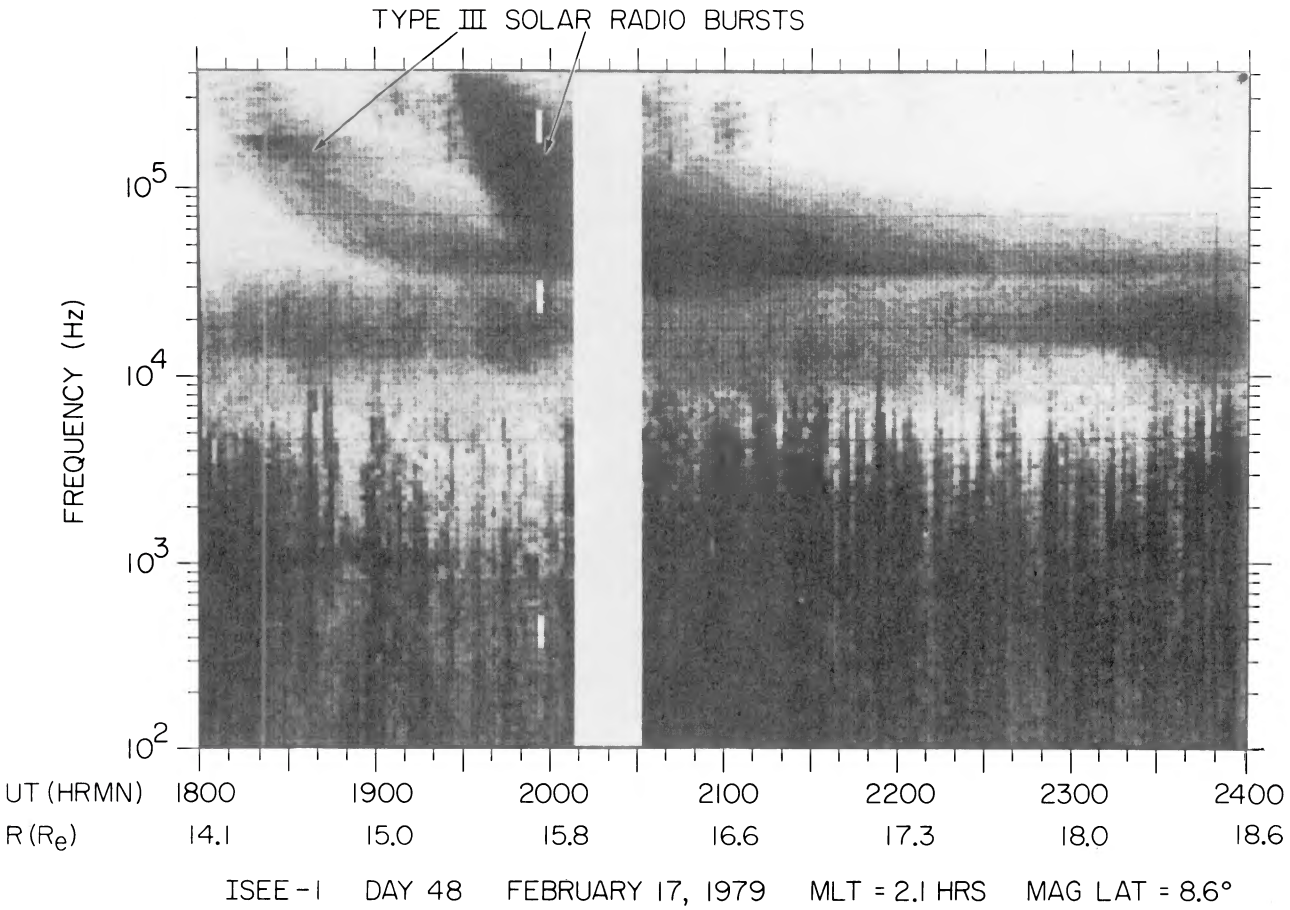

FIG. 2.—A frequency vs. time spectrogram showing the drift of two type III bursts from high to low frequencies with time

source is close to or surrounds the spacecraft. The identification of the 56.2 kHz emission as the radio emission produced near 1 AU is consistent with the (albeit uncertain) trajectory of the burst obtained through stereoscopic observations. The onset of the 56.2 kHz emission is at $\sim$ 1940 UT.

The very intense irregular electric field intensity variations in the 31.1 kHz channel from about 2000 to 2130 UT are electron plasma oscillations. Because of the filter overlap, somewhat weaker electron plasma oscillation intensities are also evident in the adjacent 17.8 and 56.2 kHz channels. The relative intensities in the adjacent channels suggest that the electron plasma frequency, f_{p-}, which is the characteristic frequency of the narrow-band electron plasma oscillations, is slightly below 31.1 kHz. This is in good agreement with the electron plasma frequency, $f_{p-} = 24$ kHz, computed using the plasma density of 7 cm^{-3} measured by the solar wind plasma instrument on *ISEE 3* (J. Gosling 1980, private communication). Thus, consistent with most previous studies of type III radiation, the 56.2 kHz radio emission identified as that produced near 1 AU is at approximately the harmonic of the plasma frequency.

The large difference between the peak and average electric field intensities indicates that the plasma oscillations are very impulsive. Figure 4 shows these plasma oscillations at the 0.5 s time resolution for 3 minutes near the maximum. The peak amplitudes appear to be limited to a level of a few mV m^{-1}. These very impulsive fluctuations are characteristic of previous observations of electron plasma oscillations associated with type III radio bursts (Gurnett and Anderson 1976, 1977). Although more intense bursts have been observed closer to the Sun (Gurnett *et al.* 1978*a*), this is one of the most intense plasma oscillation events observed at 1 AU. *Helios 2*, which was about 24° east of the Earth at the time of this event, detected only a few sporadic bursts of plasma oscillations with peak electric field strengths of only about 100 μV m^{-1}.

The bottom panel of Figure 3 shows the spin-averaged low-energy electron intensities simultaneously detected by *ISEE 3*. The solar flare electrons are first detected above 200 keV energy at about 1940 UT, the same time the 56.2 kHz in situ radio emission begins. Electrons are subsequently detected in progressively lower and lower energy channels at later and later times with very clear evidence of velocity dispersion. Simple comparison of the plasma wave and electron intensities suggests that the plasma oscillations are most clearly associated with electrons in the energy range of about 3 to 30 keV.

III. THE ELECTRON DISTRIBUTION FUNCTIONS

The University of California energetic electron experiment on the *ISEE 3* spacecraft utilizes semiconductor detector telescopes (SST) to measure electrons from 15 keV to ~ 1 MeV and an hemispherical plate electrostatic analyzer (EESA) for electrons from 2 to 18 keV. Both detector systems have fan-shaped 15° × 50° FWHM apertures viewing perpendicular to the spacecraft spin axis. As the spacecraft spins, these detectors sweep out a cone extending ± 25° from the ecliptic plane. The counts are divided into 16 sectors per spin. Since the interplanetary magnetic field generally lies near the ecliptic plane, the angular distribution of the electrons is usually obtained over all pitch angles. The EESA is stepped in 16 logarithmic energy steps from 2 to 18 keV every 64 s and provides resolution of $\Delta E/E = 12\%$. Similar resolution is obtained by the telescopes at higher energies. A malfunction in a high voltage supply limited the EESA to a maximum energy of 8.5 keV.

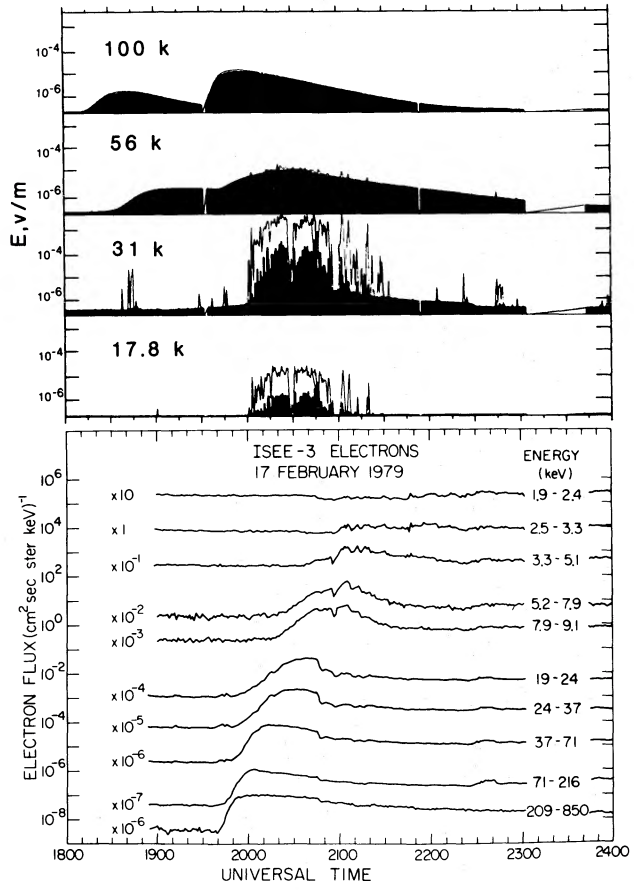

FIG. 3.—The top panel shows the electric field intensity measured from *ISEE 3* on 1979 February 17 in four broad frequency bands for the event of interest. The black areas show the intensity averaged over 64 s. The solid lines give the peak intensity measured every 0.5 s. The smoothly varying profiles in the 100 and 56.2 kHz channels show two type III radio bursts. The second one is of interest here. The intense highly impulsive emissions observed in the 31.1 and 17.8 kHz channels are the plasma waves. The lower panel shows the omnidirectional electrons from 2 keV to >200 keV. The velocity dispersion is clearly evident. No significant flux increase is observed below ~2.5 keV.

These data are used to construct the distribution of the electrons as a function of their velocity parallel to the magnetic field. We assume the electron distribution is symmetric about the magnetic field and integrated over all particles with a given $v_{\|}$ (in the following text v will represent $v_{\|}$). In the energy range 8.5–15 keV where measurements are missing, the flux level at a given energy and pitch angle has been obtained by interpolation between the fluxes measured above 15 keV and below 8.5 keV. These interpolated points affect $f(v)$ only below 15 keV. For most events, including this one, the effect on $f(v)$ is negligible a short time after the electrons below 8.5 keV begin arriving, because the event energy spectrum rises so steeply at low energies.

The resulting one-dimensional distribution functions $f(v)$ are shown in Figure 5. The solid dots in Figure 5*a* show $f(v)$ for the background population just prior to the onset of the electron event. The background population appears to consist of two distinct components with exponential distributions in v with different e-folding velocities. This type of background population of nonthermal electrons is observed at all times, although at varying flux levels. The level of this long nonthermal tail background population is important in determining when a bump will be formed in the distribution. Figure 5*a* also shows $f(v)$ every 5 minutes for the first 35 minutes of the event (1945–2015 UT). Each succeeding distribution is shifted to the right by 2×10^9 cm s^{-1} in velocity. Also, $f(v)$ is observed to develop a positive slope ($\partial f/\partial v > 0$) with time. Figure 5*b* shows $f(v)$ through the maxima in the average plasma wave electric fields (2020–2055 UT). Distributions with a region of $\partial f/\partial v > 0$ are observed from 2020 to 2045 UT. From 2045 to 2057 UT, the interplanetary magnetic field was pointed > 25° above the ecliptic plane so that small pitch angle particles could be missed by the detectors. Thus, the $f(v)$ values computed in this interval do not reflect the actual distributions. Figure 5*c* shows $f(v)$ for 2100–2135 UT. Although over most of this interval $\partial f/\partial v < 0$, there are a few short, few-minute intervals (e.g., 2100, 2105 UT) when $\partial f/\partial v > 0$.

Plasma waves with phase velocities in the range where $\partial f/\partial v > 0$ will experience Landau growth. In Figure 6 the positive values of $\partial f/\partial v$ are plotted versus time for different parallel velocities. The scale, beginning at $\partial f/\partial v = 10^{-29}$ cm^{-5} s^{-2}, is logarithmic with each tick mark indicating an increase of 1 decade. The plot for each velocity interval is placed vertically according to its range of inverse velocity. Inverse velocity is relevant because the time of arrival of a given electron energy, which determines the onset of positive $\partial f/\partial v$, is approximately inversely proportional to velocity.

The first positive $\partial f/\partial v$ is observed at ~ 1953 UT at a parallel velocity of $v \sim 1.3 \times 10^9$ cm s^{-1}. The region of positive slope drifts downward in velocity, reaching $3–4 \times 10^9$ cm s^{-1} by 2045 UT. During this time, the range of positive slope is typically $\Delta v \sim 0.3\, v$. Between 2046 and ~2056 UT, the interplanetary magnetic field is > 25° from

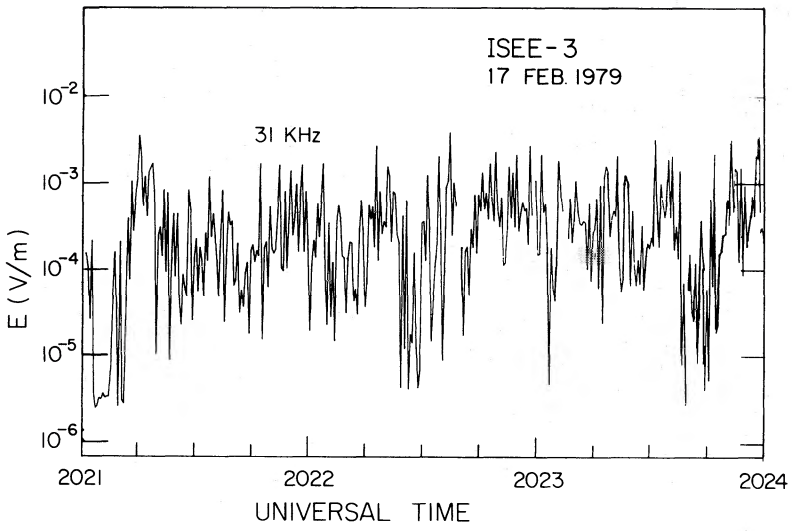

FIG. 4.—An expanded plot of the 31 kHz channel at 0.5 s resolution for 3 minutes near the maximum plasma wave intensity in the event. Note the extremely impulsive nature of the waves. The peak electric field appears to have an upper limit of 3–4 mV m^{-1}.

the ecliptic. It is possible that no positive slopes are observed because the particle experiment then does not observe small pitch angle electrons. The duration of positive $\partial f/\partial v$ at a given velocity ranges from > 10 minutes (at $v \sim 5 \times 10^9$ cm s^{-1}) to bursts of ~ 1 minute, the best time resolution of $f(v)$, with the burst behavior primarily observed at low velocities. The maximum values of $\partial f/\partial v$ range from 10^{-28} at $v \sim 1.3 \times 10^{10}$ cm s^{-1} to 10^{-24} at $v < 4 \times 10^9$ cm s^{-1}. The maximum value of $\partial f/\partial v$, regardless of velocity, rises rapidly and exceeds 10^{-27} at 1958, 10^{-26} at 2003, and 10^{-25} at 2013; and reaches a plateau at a few times 10^{-25} from 2020 to 2045 UT. Only a few isolated spikes up to 10^{-24} are observed after 2055 UT.

In general these variations in the $\partial f/\partial v$ are qualitatively mirrored by the plasma wave intensity, which rises rapidly from onset $\sim$ 2002, reaches a plateau-like maximum extending from $\sim$ 2020 to $\sim$ 2045, followed by a drop to background $\sim$ 2055 UT. Only a few spikes occur in the period 2055–2115 UT, similar behavior to that observed in $\partial f/\partial v$.

No positive slopes are observed prior to 1953 UT even though substantial fluxes of energetic electrons from this solar event are already present and a peak is already observed in the omnidirectional differential energy spectrum. Similar peaks in the energy spectrum were observed in the 1971 May 16 type III event (Lin, Evans, and Fainberg 1973). The absence of positive $\partial f/\partial v$ is due to the existence of a background electron population which is orders of magnitude larger than that of a simple 10^5 K solar wind electron distribution, and the fact that the energetic electrons have a broad angular distribution (Fig. 7). Typically at energies above $\sim$ 15 keV the FWHM of the pitch angle distribution is > 60–$80°$. In contrast, the electrons below $\sim$ 10 keV have angular FWHM of $< 25°$. Thus the 10 keV electrons are much more beamlike. This contrasting behavior of the > 15 keV and < 10 keV electrons is observed in most solar impulsive electron events. Early in the event, however, the positive slopes are produced by the > 15 keV electrons as a result of the sharp cutoff in their broad angular distributions. Later positive slopes are produced by the < 10 keV energy electrons in a one-dimensional beam, as assumed in theoretical treatments.

We have analyzed the velocity dispersion of the first arriving electrons. If electrons at all energies are released from the Sun simultaneously at t_0 and then travel along the same length L of the spiral interplanetary magnetic field line to reach the Earth, the onset time $t(\beta)$ for each velocity $\beta = v/c$ should be determined by $L/\beta c = t(\beta) - t_0$, provided the particles do not gain or lose energy on the way. This predicted linear behavior between $t(\beta)$ and β^{-1} has been observed previously, primarily above 20 keV (Lin, Evans, and Fainberg 1973). Figure 8 shows a plot of $t(\beta)$ versus β^{-1}. For points with $\beta^{-1} < 2.5$ there is a good fit to a straight line with $L = 1.31$ AU, a length consistent with the smooth spiral field line length of 1.14 AU from the Sun to the Earth, computed for the observed solar wind velocity of 360 km s^{-1} (J. Gosling 1980, private communication). For $\beta^{-1} > 2.5$, however, the points fall below the line, and at $\beta^{-1} > 5$ the points fit to a line with $L = 0.92$ AU, far less than the smooth Sun-Earth field line length.

This analysis suggests that the electrons below $\sim$ 50 keV may have lost substantial amounts of energy in traveling from the Sun to 1 AU. This velocity range is just that in which positive slopes in $f(v)$ are observed. Thus, a consistent interpretation of these data is that these electrons are losing energy to plasma waves by the process of Landau growth.

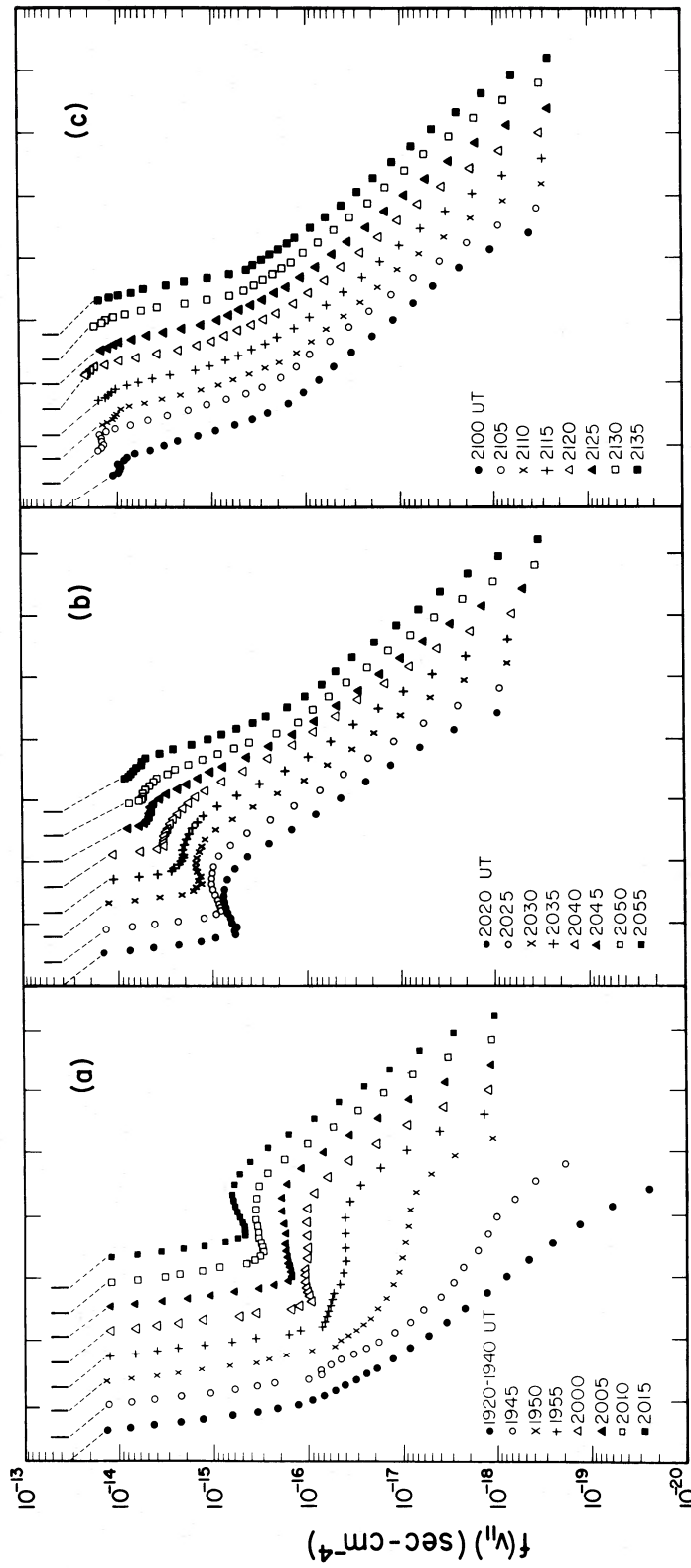

FIG. 5.—The comprehensive measurements over energy and angle taken from *ISEE 3* on 1979 February 17 have been used to construct the one-dimensional velocity distribution function of the electrons every 64 s. The distribution averaged over 20 minutes prior to the event onset is indicated by the solid dots in panel (*a*). The 64 s measurements of the distribution during the event are shown every 5 minutes. Note the positive slope which develops and moves to lower velocities with time. During the interval ~2045–2055 UT the measurements are incomplete because the magnetic field is not contained in the electron detectors' field of view. After 2100 UT positive slopes are only infrequently observed in the distribution.

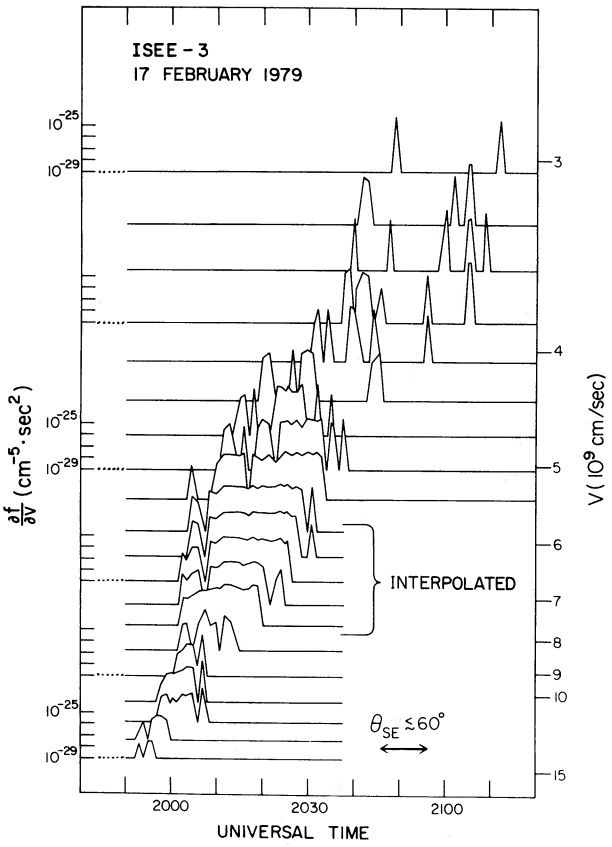

FIG. 6.—For each velocity interval the value of the positive slope $\partial f/\partial v$ is plotted here vs. time. The velocity is given by the right-hand scale. The slope $\partial f/\partial v$ is plotted on a logarithmic scale, indicated on the left-hand side. Each tick mark is one of magnitude starting at 10^{-29} cm^{-5} s^{-2}. The shift of the region of positive slope to lower velocities with time is due to velocity dispersion. The velocity range over which interpolations of the electron data are used is indicated. The interplanetary magnetic field is out of the electron detectors' field of view during the interval marked $\Theta_{se} \lesssim 60°$. During this time the distribution functions are incompletely sampled.

IV. DISCUSSION

The observations can be summarized as follows:

1. A bump on tail distribution is produced by the dispersion in velocity of the electrons. Positive $\partial f/\partial v$ begins substantially later than the first arrival of the electrons, however, because of the background electron distribution and the broad angular distributions ($> 60°$ FWHM) of the > 15 keV electrons.

2. In contrast, the < 10 keV electrons are highly beamlike, $< 25°$ FWHM. Large positive $\partial f/\partial v$, however, is produced by both the broad angular distribution at high energies and the beamlike lower energy electrons.

3. Positive slopes are observed at parallel velocities of from 1.3×10^{10} cm s^{-1} to 3×10^9 cm s^{-1}. Typical values for $\partial f/\partial v$ range from 10^{-28} cm^{-5} s^{-2} at high velocities to 10^{-24} at low velocities. At a given time, the region of positive slopes covers $\Delta v/v \sim 0.3$.

4. Strong positive slopes $\partial f/\partial v \approx 10^{-25}$ cm^{-5} s^{-2} are observed to persist for periods of > 10 minutes. Thus, there is no rapid plateauing of the distribution.

5. There is evidence that the electrons below ~ 50 keV, in the velocity range for which positive $\partial f/\partial v$ is observed, lose significant amounts of energy in traveling from the Sun to 1 AU.

6. The plasma wave intensity is qualitatively closely correlated with variations in $\partial f/\partial v$.

7. The plasma waves are highly impulsive, and there appears to be a maximum level of a few mV m^{-1}.

8. The 56.2 kHz radio emission, identified as that produced near the spacecraft, begins simultaneously with the arrival of the first electrons and ~ 20 minutes before the plasma wave onset.

Neglecting spontaneous emission and collisional damping, the growth of the plasma waves can be described in one dimension by

$$\frac{\partial P}{\partial t} = \gamma P(k, z, t) ,$$

where

$$\gamma = \frac{4\pi^2 e^2 v^2}{\omega m} \left.\frac{\partial f}{\partial v}\right|_{v=\omega/k} ,$$

and $P(k, z, t)$ is the plasma wave energy distribution in wave number k (Magelssen and Smith 1977). For positive $\partial f/\partial v$, P grows by a factor $\exp(\int \gamma dt)$. For this event $\omega \approx 1.5 \times 10^5$ s^{-1}, and $v \approx 10^{10}$ cm s^{-1} near onset, so

$$\int \gamma dt = 7 \times 10^{24} \int \left.\frac{\partial f}{\partial v}\right|_{v=\omega/k} dt .$$

At the observed plasma wave onset, ~ 2003 UT, the average electric field intensity jumps up by greater than a factor of 10^2 above background levels, implying P increases by a factor of 10^4, and therefore $\int \gamma dt = 10$. (If instead of using the observed background levels we use the equilibrium plasma wave levels computed for the observed electron background distribution, we get a comparable value for $\int \gamma dt$.) From Figure 7 we find that $\int \gamma dt$ reaches values of 10 at 2003–2004 UT, in excellent agreement with the plasma wave onset. The continued increase up to 2025 UT is qualitatively matched by the increase in both maximum and average plasma wave levels. Also the isolated bursts after 2100 UT appear related to short isolated intervals of positive $\partial f/\partial v$.

The large positive values of $\partial f/\partial v > 10^{-25}$ cm^{-5} s^{-2} observed after ~ 2015 UT give $\gamma < 1$ s^{-1}. Since $\partial f/\partial v$ persists at these levels for minutes at a given velocity, linear theory would predict plasma wave levels many orders of magnitude above what is observed. It is possible, but very unlikely, that plasma waves are present at these predicted levels and not observed. If the plasma waves are confined to regions much smaller than ~ 20 km, they would be convected past the spacecraft in times much less than 50 ms, the time constant of the receivers. As a result, the plasma wave instrument would highly attenuate or even completely miss the wave electric fields.

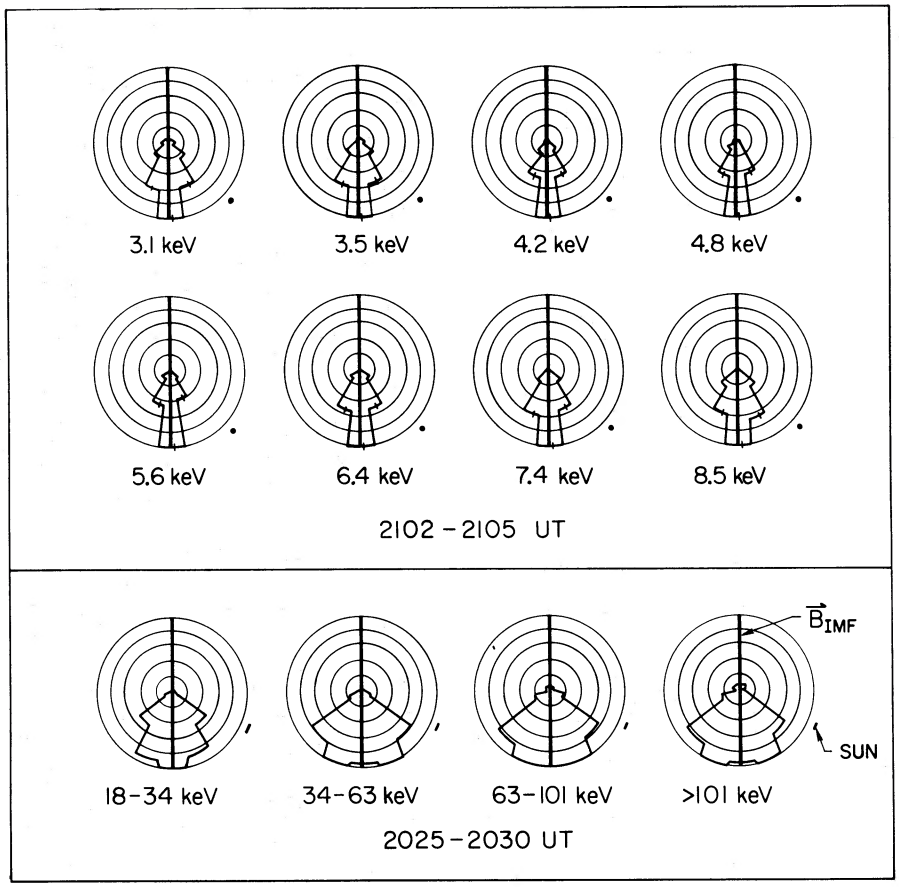

FIG. 7.—Polar plots of the pitch angle distributions for electrons in different energy intervals measured from *ISEE 3* on 1979 February 17. Note the broad, >90° FWHM, flat-topped and sharp-sided distributions at energies above ~20 keV, as compared with the one-dimensional <25° FWHM beamlike character at low energies.

Provided this is not the situation here, however, these electron distributions would imply that some process must be limiting the plasma wave growth. One possibility is that the waves could be removed from resonance as they propagate through the density fluctuations in the solar wind. (G. de Genouillac 1980, and, independently, M. Goldman 1980, private communications). Also several nonlinear processes [decay instability, OTSI (oscillating two stream instability), soliton collapse, etc.] have been suggested as mechanisms to limit wave growth and also to shift the waves out of resonance with the beam. We note here that such nonlinear processes are predicted to occur for conditions at 1 AU at a wave threshold of ~ 10 mV m^{-1} (D. R. Nicholson 1980, private communication). This is close to the maximum plasma wave levels observed (Fig. 4).

The impulsive nature of the plasma waves suggests that some process is bunching them. Density fluctuations present in the ambient solar wind may be important for bunching the waves and perhaps for helping the soliton collapse process. If soliton collapse occurs, extremely small regions ($L \sim 10\lambda_D \sim 100$ m) of intense plasma waves should be created. These would be convected past the spacecraft too fast to be observed by the plasma wave detector. After soliton collapse, however, the waves should disperse into a larger region which could be observed. The impulsive nature of the plasma waves may be the signature of the remnants of the collapsed solitons.

We now consider the quasi-linear diffusion of the electrons in velocity space by the plasma waves. This can be described, under the same assumptions as before, by

$$\frac{\partial f}{\partial v} = \frac{2\pi e^2}{m}\frac{\partial}{\partial v}\left[\frac{P(k=\omega/v)}{v}\frac{\partial f}{\partial v}\right] = \frac{2\pi e^2}{m}\left[P\left(v\frac{\partial^2 f}{\partial v^2} - \frac{\partial f}{\partial v}\right) + v\frac{\partial f}{\partial v}\frac{\partial P}{\partial v}\right].$$

Assuming that the waves are contained in a cone of half angle $\sim 20°$ about the B field direction (Magelssen and Smith 1977), we obtain $P = 2.9 \times 10^{-8}E^2/\Delta k$ (cgs), where E is the wave electric field in v/m. Since we do not know the spectral shape of P, we will estimate $\partial f/\partial v$ by neglecting the last term. Defining the time constant for diffusion as $\tau_D = |f(\partial f/\partial v)^{-1}|$, we find for times near plasma wave maximum ($\sim$ 2025 UT)

$$\tau_D(\mathrm{s}) = 7 \times 10^{-6}E(v/m).$$

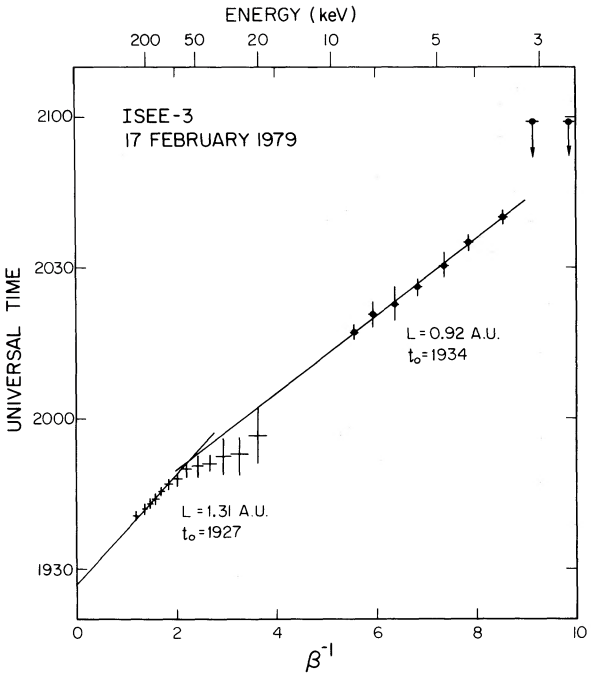

FIG. 8.—Plotted here is the time of onset of the electrons in different energy intervals vs. the increase of their velocity. If electrons at all energies were released simultaneously at t_0 and traveled the same distance L, we would obtain a straight line. For high energies $\beta^{-1} < 2.5$ a good fit to a straight line is obtained with reasonable values for L and t_0. The lower energy electrons, however, arrive far too early. This could be explained if they started at a higher energy but lost energy to plasma waves in traveling to 1 AU.

At 2025 UT, the peak electric field is ~ 5 mV m^{-1} and the average is ~ 0.3 mV m^{-1}, giving $\tau_D = 0.15$ and 80 s, respectively. The plasma waves appear spiky even at the highest time resolution of 0.5 s, implying regions of scale size less than 200 km convected along by a 400 km s^{-1} solar wind. The fast electrons ($v = 5 \times 10^{-9}$ cm s^{-1}) will traverse one of these intense wave regions in times less than 4×10^{-3} s. Thus, the velocity diffusion that occurs in one of these regions is insufficient to plateau the electron distribution, and the diffusion in velocity may be better described as the average effect of these short-lived encounters. For comparison at $v \sim 4$–5×10^9 cm s^{-1}, $\partial f/\partial v$ remains positive for ~ 10 minutes, many times τ_D. The fact that there is no obvious strong plateauing suggests that observed plasma waves may have been shifted in k space by the above-mentioned processes, so they are no longer resonant with the electrons.

The observed distribution functions thus provide evidence that some process is occurring which limits the wave growth and shifts the waves out of resonance with the beam electrons. Although this process reduces the energy lost by the electrons as they travel out of the Sun, the analysis of the electron velocity dispersion suggests that the electrons have still lost a significant fraction of their energy to plasma waves through Landau damping.

We turn now to the radio emission. Figure 3 shows that the 56.2 kHz emission identified as in situ begins simultaneously with the first arrival of the fast electrons, and clearly precedes the onset of the plasma waves by ~ 20 minutes. We have found more than a dozen other events for which uncontaminated electron, plasma wave, and radio data are available from *ISEE 3*. In all these events the sequence of electrons, radio, and plasma waves is the same as presented here. The most energetic electrons arrive simultaneously with the onset of the radio burst, with the plasma waves beginning typically 15–40 minutes later at the time of arrival of the < 25 keV electrons. The radio emission and most energetic electrons are found to begin simultaneously in previous studies as well (Alvarez, Haddock, and Lin 1972; Lin, Evans, and Fainberg 1973). Furthermore, the radio flux, J_r, is observed to be related to the total electron flux, J_e, by $J_r \propto J_e^{\alpha}$, where $\alpha \approx 1$ at low electron fluxes, changing to $\alpha \approx 2.5$ at higher electron fluxes (Fitzenreiter, Evans, and Lin 1976). This kind of quantitative relationship suggests that the in situ radio emission is closely related to the energetic electrons.

The delay, then, of $\sim$ 15–40 minutes between the onset of the in situ radio emission and the onset of the plasma waves is difficult to reconcile with the commonly held hypothesis that the plasma waves are the sources of the radio emission. In the event studied here, 56.2 kHz is the first emission frequency to show no directivity, i.e., no spin modulation. Because type III radio sources are usually quite large (viewed from the Sun, the sources typically subtend $\sim 60°$ in angle), there may be no spin modulation even when the source is one- or two-tenths of an AU away from the spacecraft. In the absence of significant amounts of scattering of the radio emission, we estimate that the 56.2 kHz source must be located no further than 0.2 AU from the spacecraft. Plasma waves at levels substantially above background must therefore be present at > 0.8 AU at 1940 UT, yet we do not observe plasma waves at 1 AU until ~ 20 minutes later. This leads to a propagation velocity for the front edge of the plasma wave region of $< 0.1\ c$ between 0.8 and 1 AU, compared to an average velocity for the radio event of $\sim 0.3\ c$ from the Sun to 1 AU. The latter velocity is typical of most type III bursts. In previous studies little, if any, deceleration is observed for type III bursts in traveling from the Sun to 1 AU, and certainly no abrupt deceleration of the kind suggested by this delay.

We have investigated several other possible explanations for the delay:

1. The 56.2 kHz radio emission may actually come from much closer to the Sun, say at ~ 0.5 AU, where plasma waves are present at the time of radio onset. Significant scattering of the radio emission from density inhomogeneities around the spacecraft may produce the effect of isotropizing the radiation. The radio emission could then be at the fundamental of the plasma frequency (see Kellogg 1980).

2. Plasma waves are present at 1 AU at the 56.2 kHz radio onset but for various reasons are not observed. Since the measurements of the plasma waves and electrons are made at only one point in space while the radio

emission is received from a large volume, we cannot rule out various inhomogeneous theories for explaining the delay, i.e., the "raisin bread" hypothesis, where the plasma waves producing the early radio emission are restricted to a few small regions which are missed by the spacecraft. These explanations become less likely, however, as more events are observed.

Another possibility is that the plasma waves which produce the early radio emission are confined to very small regions, < 20 km, which may be missed by the plasma wave instrument. For waves resonant with the electron velocities of $\sim 10^9$–10^{10} cm s^{-1}, k is $\sim 10^{-4}$–10^{-5} or $\lambda \sim 0.1$–1 km. Thus, regions of 10–100 λ size could be missed. Since plasma waves are observed later in the event, possibly very small wave packets are produced initially which expand with time or with additional growth. The quasi-linear computation based on the observed $f(v)$, however, predicts intense plasma waves will not be generated in the 1979 February 17 event until $\sim$ 2003 UT, when they are in fact observed.

3. The type III radio emission may be produced by a completely different mechanism having nothing to do with the plasma waves. This mechanism may predominantly involve electrons which are more energetic than those producing the plasma waves. A mechanism involving direct conversion of particle energy into electromagnetic energy could be much more efficient. In support of this possibility, we note that *ISEE 3* has observed a few impulsive solar electron events in which the electron fluxes at low energies, $\lesssim 20$ keV, did not increase above pre-event background. In those events the radio emission was observed with the same close relationship to the fast electrons as in the other events, but no plasma waves were observed at all.

V. CONCLUSIONS

The observations reported here clearly show that the plasma waves observed in association with many type III bursts are generated by $\sim$ 3–50 keV electrons. The bump on tail distribution functions which are unstable to the growth of Langmuir waves are produced both by the sharply confined 60–80° FWHM distributions of the high energy electrons and by the beamlike low energy electrons. These distributions remain unstable at a given velocity for long enough times to drive the plasma waves well above the maximum observed level of 3–4 mV m^{-1}. Thus, some process must be limiting the plasma wave growth. We note that these levels are at about the threshold for nonlinear processes such as OTSI, soliton collapse, etc. Such nonlinear processes could provide an upper limit to the plasma wave intensity by shifting the plasma waves out of resonance with the beam electrons, thus allowing the electrons to propagate from the Sun to beyond 1 AU without catastrophic energy losses. Another possibility is that density fluctuations in the solar wind may remove the waves from resonance with the beam.

The relationship of the plasma waves to the radio emission is unclear. If there is substantial scattering of the radio waves in the interplanetary medium, then a model where the radio emission is generated at the fundamental by the plasma waves would be consistent with the data. We believe, however, the observations provide substantial impetus to examine mechanisms for producing type III emission which do not involve plasma waves.

R. P. L. acknowledges useful discussions with G. de Genouillac, G. Dulk, M. Goldman, and D. Nicholson. The research at Berkeley was supported in part by NASA contract NAS-5-22307. The research at the University of Iowa was supported by NASA through contracts NAS5-20093, NAS5-26125, and NAS5-11279 with Goddard Space Flight Center and by grants NGL-16-001-002 and NGL-16-001-043 with NASA Headquarters. The research at TRW was supported by NASA through contract NAS5-20682.

REFERENCES

Alvarez, H., Haddock, F. T., and Lin, R. P. 1972, *Solar Phys.*, **26**, 468.
Anderson, K. A., Lin, R. P., Potter, D. W., and Heetderks, H. D. 1978, *IEEE Trans. Geosci. Elect.*, **GE-16**, 153.
Bardwell, S., and Goldman, M. V. 1976, *Ap. J.*, **209**, 912.
Fitzenreiter, R. J., Evans, L. G., and Lin, R. P. 1976, *Solar Phys.*, **46**, 437.
Frank, L. A., and Gurnett, D. A. 1972, *Solar Phys.*, **27**, 446.
Ginzburg, V. L., and Zheleznyakov, V. V. 1958, *Sov. Astron.—AJ*, **2**, 653.
Goldstein, M. L., Smith, R. A., and Papadopoulos, K. 1979, *Ap. J.*, **234**, 683.
Gurnett, D. A. 1974, *J. Geophys. Res.*, **79**, 4227.
Gurnett, D. A., and Anderson, R. R. 1976, *Science*, **194**, 1159.
———. 1977, *J. Geophys. Res.*, **82**, 632.
Gurnett, D. A., Anderson, R. R., Scarf, F. L., and Kurth, W. S. 1978*a*, *J. Geophys. Res.*, **83**, 4147.
Gurnett, D. A., Scarf, F. L., Fredricks, R. W., and Smith, E. J. 1978*b*, *IEEE Trans. Geosci. Elect.*, **GE-16**, 225.
Kaplan, S. A., and Tsytovich, V. N. 1968, *Sov. Astron.—AJ*, **11**, 956.
Kellogg, P. J. 1980, *Ap. J.*, **236**, 696.
Lin, R. P. 1970, *Solar Phys.*, **12**, 266.
Lin, R. P. 1974, *Space Rev.*, **16**, 189.
Lin, R. P., Evans, L. G., and Fainberg, J. 1973, *Ap. Letters*, **14**, 191.
Magelssen, G. R., and Smith, D. F. 1977, *Solar Phys.*, **55**, 211.
Nicholson, D. R., Goldman, M. V., Hoyng, P., and Weatherall, J. S. 1978, *Ap. J.*, **223**, 605.
Papadopoulos, K., Goldstein, M. L., and Smith, R. A. 1974, *Ap. J.*, **190**, 175.
Parker, E. N. 1958, *Ap. J.*, **128**, 664.
Scarf, F. L., Fredricks, R. W., Gurnett, D. A., and Smith, E. J. 1978, *IEEE Trans. Geosci. Elect.*, **GE-16**, 191.
Smith, D. F. 1977, *Ap. J. (Letters)*, **216**, L53.
Smith, R. A., Goldstein, M. L., and Papadopoulos, K. 1979, *Ap. J.*, **234**, 348.
Sturrock, P. A. 1964, *AAS-NASA Symposium on the Physics of Solar Flares*, ed. W. N. Hess (NASA SP-50), p. 357.
Takakura, T., and Shibahashi, H. 1976, *Solar Phys.*, **46**, 323.
Tidman, D. A., Birmingham, T. J., and Stainer, H. M. 1966, *Ap. J.*, **146**, 206.

D. A. GURNETT: Department of Physics and Astronomy, University of Iowa, Iowa City, IA 52242
R. P. LIN and D. W. POTTER: Space Sciences Laboratory, University of California, Berkeley, CA 94720
F. L. SCARF: TRW Defense and Space Systems, Redondo Beach, CA 90278